Analysis of spaced-antenna retrieval precision using an X-band active phased-array weather radar

V. Venkatesh[1], K. Orzel[2], T. Hartley[2], and S.J. Frasier[2]

[1] *Pacific Northwest National Lab, Richland, WA 99352, USA*

[2] *Microwave Remote Sensing Laboratory, University of Massachusetts, Amherst, MA 01003, USA*

ABSTRACT

Spaced-antenna retrievals are a potential means of higher spatial-resolution wind-field retrievals than currently available single radar algorithms in the weather radar community. Relevant literature to date has either been theoretical (Zhang and Doviak (2007)) or based on simulations ((Venkatesh and Frasier (2013)). On a dataset with smoothly varying wind-profiles, spaced-antenna (SA) measurements are compared to Doppler beam swinging (DBS) and Velocity Azimuth Display (VAD)-like variational retrievals of baseline wind. Qualitative features of the G-SZl, FSA, DBS and VAD retrievals are shown to be consistent.

1. Introduction

Since the first use of Doppler weather radars (Probert-Jones (1960)), research on radar algorithms and technology have continuosly improved their performance (Seliga and Bringi (1976), Bharadwaj et al. (2010), Chandrasekar et al. (2013)). The advent of phased-array weather radars have enabled several new capabilities (Zrnić et al. (2007)). Some examples follow. The ability of phased-array radars to "multiplex" between locations has improved data quality, when the echo coherence time is comparable to the dwell time (Yu et al. (2006)). Kalman filtering techniques to assimilate data over shorter time-scales (Yossouf and Stensrud (2010)) and adaptive signal processing techniques for imaging precipitation events have been demonstrated (Isom et al. (2013)).

This work focusses on a high spatial-resolution technique for wind-field retrieval using phased-array radar technology. The SA method was originally developed to profile plasma inhomogeneities in the Ionosphere and has since been succesfully employed for clear-air observations of the convective boundary layer. Interest in applying this method to profile precipitation is relatively recent. To date, iterature on spaced-antenna weather radars has either been theoretical (Zhang and Doviak (2007), Zhang and Doviak (2008)) or based on numerical simulations (Venkatesh and Frasier (2013)). Although Hardwick et al. (2005) have documented spaced-antenna observations earlier, empirical studies evaluating the precision of SA retrievals on precipitation echoes have not been reported.

Herein, we evaluate the precision of spaced-antenna retrievals on precipitation echoes using data collected with an X-band phased-array weather radar. "VAD-like" variational retrievals and Doppler beam swinging retrievals are used as prognostics. In the following section, we describe the spaced-antenna implementation, the experimental setup and data processing methodology. We then describe the dataset and present a comparitive analysis of the retrieval algorithms considered.

2. Methods and results

a. *Instrument description*

The Univerisity of Massachusetts has developed an active phased-array radar system capable of electronic scanning along azimuth (Orzel et al. (2013), Orzel et al. (2011), Hopf et al. (2009)). The system comprises of a linear array antenna, programmable Transmit- receive (T/R) modules, a master FPGA controller and a host computer. The antenna consists of 64 "stick" elements, where each stick is a series-fed microstrip patch column. The full array has a 1.6 degree beamwidth at broadside in the azimuth plane and a 3.5 degree beamwidth in the elevation plane. Behind each antenna stick, T/R modules provide independent control of amplitude and phase. The T/R modules are synchronized by clocking signals provided by master FPGA controller. In turn, the timing register in this master controller are populated by a beam scheduling application in the host computer. The concept for spaced-antenna operation is to use alternating apertures with displaced

Table 1: X-band phased array spaced antenna syste,.

Pulse repetition frequency	5 kHz
Effective spaced antenna baseline	8 cm
Equivalent azimuthal 3-dB beamwidth	2.7 degrees
Dwell time	1.8 seconds
Radar frequency	9.36 GHz

phase-centers on receive (Venkatesh and Frasier (2013), Venkatesh and Frasier (2011)). Although a 5 degree aperture would have been most optimal for SA retrievals at X-band, we found that RF beamforming errors become more pronounced with reducing aperture size. Consequently, a 2.7 degree spaced-antenna system is used herein. The aperture size and left-right sub-array phase center displacement are increased with electronic scan-angle to compensate for the "cosine roll-off". This fixes the radar resolution and the SA baseline, thereby simplifying data-analysis and interpretation. The implemented spaced-antenna system is summarized in Table 1.

b. Data processing methodology

For the executed experiment to compare spaced-antenna retrievals to Doppler beam swinging and VAD-like variational retrievals of baseline wind, the antenna motion is in discrete steps of 5 degrees, such that there is no mechanical slew during the duration of the dwell. During each dwell of 1.8s, interleaved I/Q data from the left and right-sub arrays are logged. Using this data, spaced-antenna retrievals of baseline wind are compared to existing coarser azimuthal-resolution baseline-wind retrievals. Monte-Carlo based simulations (Venkatesh and Frasier (2013), **?**) are used to validate the algorithm implementations and synthesize processing thresholds for data-analysis. For every beam location, complex I/Q data is read and stored in a 2-D array. The two dimensions of this array correspond to "fast-time" (range) and "slow-time" (pulse number). The I/Q data is first compressed in fast time using standard matched filtering and windowing methods. Following this the data is "de-interleaved" to separate pulses corresponding to left and right apertures. Auto-/Cross- spectra and correlation functions are then estimated to yield moments and retrievals.

The DBS method retrieves the wind-field directly from two radial velocity observations (denote by $\widehat{v}_{r1}$ and $\widehat{v}_{r2}$ respectively) separated by some scan angle ϕ_{DBS}. The cross-beam wind is then retrieved from

$$\widehat{v}_{DBS} = \widehat{v}_{r1}\tan\phi_{DBS} + \frac{\widehat{v}_{r2} - \frac{\widehat{v}_{r1}}{\cos\phi_{DBS}}}{\sin\phi_{DBS}} \tag{1}$$

where, $\widehat{v}_{DBS}$ denotes the DBS retrieval.

The variational method retrieves the mean wind-field from a least squares fit to radial velocity observations (Laroche and Zawadski (1994), Shapiro et al. (2006)). The precision of the resultant estimate depends on the cost function employed. Herein, the implemented cost function retrieves the wind-field from an estimates of the first and second harmonics of radial velocity. For N looks at an analysis volume, let the radial velocity estimates be represented as $\widehat{v}_{r_n}$ and fits to the radial velocity observations be $v_{r_{fit}}$. Let the corresponding azimuthal angles be represented by ϕ_n, where $n = 1, 2, 3, ..., N$.

$$v_{r_{fit}} = \widehat{a}_0 + \widehat{a}_1\cos(\widehat{\Omega}_1 + \phi_n) + a_2\cos(\widehat{\Omega}_2 + 2\phi_n) \tag{2}$$

In matrix form, this becomes

$$\left[v_{r_{fit}}\right] = \left[\begin{array}{cc} 1\cos(\widehat{\Omega}_1 + \phi) & \cos(\widehat{\Omega}_2 + \phi) \end{array}\right] \left[\begin{array}{c} \widehat{a}_0 \\ \widehat{a}_1 \\ \widehat{a}_2 \end{array}\right] \tag{3}$$

Here $\widehat{a}_0$, $\widehat{a}_1$ and $\widehat{a}_2$ are the estimated magnitudes of the zeroth, first and second harmonic respectively. The symbols $\widehat{\Omega}_1$ and $\widehat{\Omega}_2$ are the phases corresponding to the first and second harmonics. The wind-field is paramterized by the finding values $a\widehat{a}_0$, $\widehat{a}_1$, $\widehat{a}_2$, $\widehat{\Omega}_1$ and $\widehat{\Omega}_2$ that minimize the cost function. Specifically,

$$J = \left\{ \left[v_{r_n}\right] - \left[v_{r_{fit}}\right] \right\}^2 \tag{4}$$

Note that some authors use the number "$\frac{1}{2}$" in the cost function. This is typically done for ease of working with the derivatives of J. However, our implementation synthesizes a mesh of discrete values of a_0, a_1, a_2, Ω_1 and Ω_2, calculates J throughout this mesh and picks values that correspond to its minimum. Although computationally inefficient, this "brute force" approach serves as a prognostic to visualize solution uniqueness. Finally, the mean baseline wind is retrieved as

$$\widehat{v}_{VAD-baseline} = \widehat{a}_1 sin(\widehat{\Omega}_1 + \phi_n) + \widehat{a}_2 sin(\widehat{\Omega}_2 + \phi_n) \tag{5}$$

Note that the zeroth harmonic is omitted from the VAD-like retrieval of baseline wind. This is because both knowm mechanisms that contribute to the zeroth harmonic (hydrometeor fall velocity and wind-field divergence) are orthogonal to the baseline wind.

c. Qualitative comparisons

Fig. dataset shows observations of a convective rain event at an elevation of 20 degrees in Amherst, MA on July, 23rd, 2013. Due to beam blockage issues, the maximum coverage was limited to 265 degrees. Fig. 1a shows FFT-based radial velocity estimates on the storm. Here, negative radial velocities indicate motion towards the radar. Qualitatively, the spatial variation of radial velocity on this dataset appear consistent with well known signatures in Wood and Brown (196). Fig. 1b shows FFT-based estimates of spectrum width. Note the region of large spectrum width at a range of about 10 Km, albeit its interpretation is ambiguous in the absence of reflectivity or dual-polarization products. Since the calibration precision of the phased-array radar system was not quantified at the time of this, we refrain from interpreting the reflectivity signature. Fig. 1c-d show that the SNR at the left and right sub-arrays is nearly identical. This, along with antenna pattern and baseline measurements provided in Venkatesh (2013), provide confidence in the spaced-antenna implementation.

Fig. 2a-d ahow that the G-SZL and FSA retrievals are in qualitative agreement with the DBS and VAD-like variational retrievals of baseline wind. To produce Fig. 2c-d, we have matched the azimuthal resolution of the spaced-antenna (G-SZL and FSA) retrievals by running a 3-point moving average filter in azimuth. An additional 3-point smoothing in range was performed on all baseline retrievals methods. From Fig. 2 we see that the VAD-like retrievals of large scale baseline wind, DBS retrievals, G-SZL and FSA retrievals are qualitatively consistent.

3. Summary

Herein, we presented a qualitative evaluation of spaced-antenna retrievals using a weather radar. The executed experiment to compare SA retrievals to DBS and VAD-like variational retrievals utilized stepped motion of the beam such that there was no slewing during the dwell. On a dataset with smoothly varying wind-profiles, the SA retrievals were in qualititative agreement with the DBS and VAD method. Quantitative analysis efforts are ongoing.

The methodology employed in this work was reliant on a dataset with smooth wind-profiles and low wind-speeds. Based on results obtained on this dataset, spaced-antenna retrievals appear possible with weather radars at close range for low to moderate wind-speeds. A future study using spaced-antenna retrievals as a constraint for variational retrievals using dual-Doppler retrievals as ground truth is planned.

REFERENCES

Bharadwaj, N., V. Chandrasekar, and F. Junyent, 2010: Signal processing system for the casa ip1 project radars. *J. Atmos. Oceanic. Tech.*, **27**, 1440–1460.

Chandrasekar, V., R. Keranen, S. Lim, and D. Moisseev, 2013: Recent advances in classification of observations from dual-polarization weather radars. *Atmospheric Research*, **119**, 97–111.

Hardwick, K., S. Frasier, A. Pazmany, H. Bluestein, and M. French, 2005: Spaced antenna measurements of cross beam velocity in severe storms. *32nd Conference on Radar Meteorology*, AMS, Albuquerque, NM, P4R.11.

Hopf, A. P., J. Salazar, R. Medina, V. Venkatesh, E. Knapp, S. Frasier, and D. McLaughlin, 2009: Casa phased-array radar system description, simulation and products. *Int'l. Geosci. & Remote Sensing Symposium*, IEEE, Boston, MA.

Isom, B., et al., 2013: The atmospheric imaging radar : Simultaneous volumetric observations using a phased array weather radar. *J. Atmos. Oceanic. Tech.*, **30**, 655–675.

Laroche, S. and I. Zawadski, 1994: A variational analysis method for retrieval of three-dimensional wind-field from single doppler radar data. *J. Atmos. Oceanic. Tech.*, **51**, 2664–2682.

Orzel, K., V. Venkatesh, T. Hartley, and S. Frasier, 2013: Development and calibration of a x-band dual polarization phased array radar. *Proceedings of IEEE Radar conference*, IEEE, Ottawa, Canada.

Orzel, K., et al., 2011: Mobile x-band dual-polarization phased-array radar: Systems requirements and development. *35th Conference on Radar Meteorology*, AMS, Pittsburgh, PA, 14.A4.

Seliga, T. A. and V. N. Bringi, 1976: Potential use of radar differential reflectivity measurements at orthhogonal polarizations for measuring precipitation. *J. Appl. Meteor.*, **15**, 69–75.

Shapiro, A., P. Robinson, J. Wurman, and J. Gao, 2006: Single Doppler velocity retrieval with rapid-scan radar data. *J. Atmos. Oceanic. Tech.*, **20**, 1758–1777.

Venkatesh, V., 2013: *Spaced-antenna wind estimation using an X-band active phased-array weather radar*. PhD dissertation, University of Massachusetts.

Venkatesh, V. and S. Frasier, 2011: Design considerations for an x-band spaced-antenna weather radar. *34th Conference on Radar Meteorology*, AMS, Williamsburg, VA, 9.A6.

Venkatesh, V. and S. Frasier, 2013: Simulation of spaced-antenna wind retrieval performance for an x-band phased-array weather radar. *J. Atmos. Oceanic. Tech.*, **30**, 1447–1459.

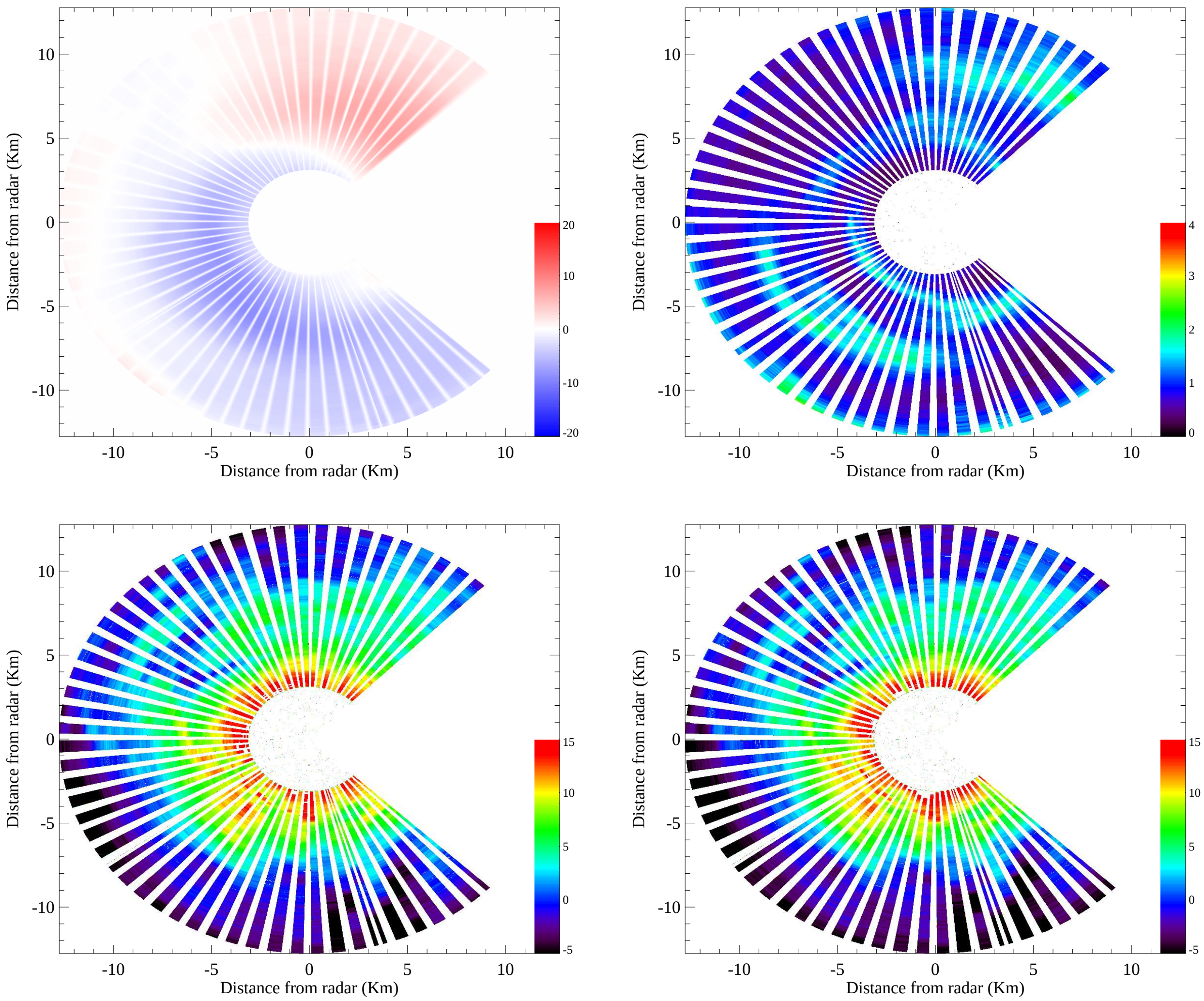

Figure 1: Measurements from a convective storm on August 26^{rd}, 2013 in Amherst, MA using "stepped" mechanical scanning at 10 degrees elevation. Data is shown in wedges to reflect discrete and discontinuos sampling in azimuth. Clockwise from top left. (a) - FFT based radial velocity estimates Negative velocities indicate motion towards the radar. (b) - FFT based spectrum width estimates. (c) - Left sub-array SNR measurements. (d) - Right sub-array SNR measurements. In Fig. (a), negative velocities indicate motion towards the radar.

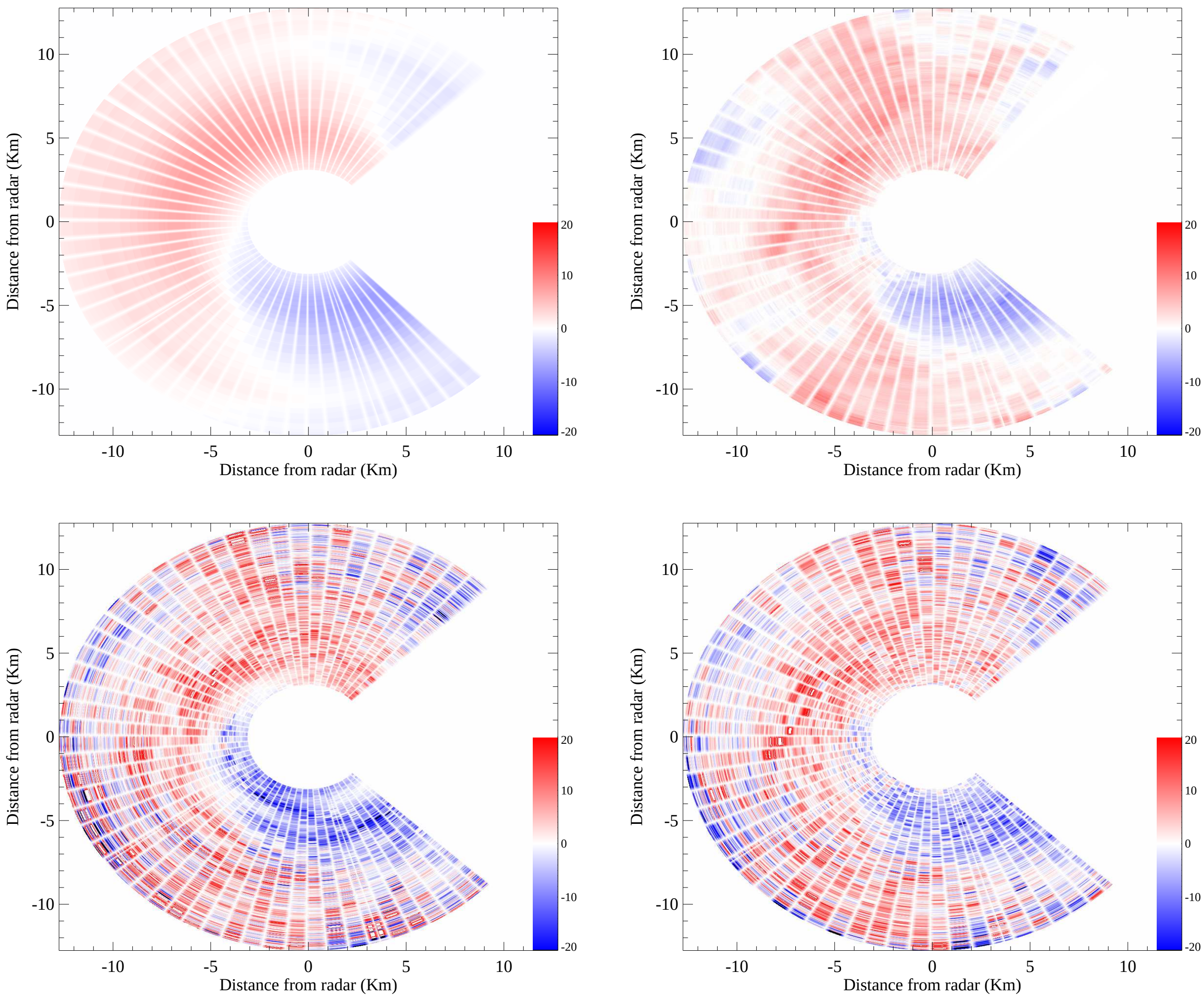

Figure 2: Baseline wind measurements at an elevation of 20 degrees. Clockwise from top left. (a) - VAD-like variational retrievals of baseline wind. (b) - DBS retrievals (c) - Spaced antenna retrievals using the FSA algorithm. (d) - Spaced-antenna retrievals using the G-SZL algorithm. Positive velocities indicate clockwise motion.

Wood, V. T. and R. Brown, 196: Single doppler velocity signature interpretation of non-divergent environmental winds. *J. Atmos. Oceanic. Tech.*, **3**, 114–128.

Yossouf, N. and D. J. Stensrud, 2010: Impact of phased-array radar observations over a short assimilation period: Observing system simulation experiments using an ensemble kalman filter. *J. Atmos. Oceanic. Tech.*, **138**, 517–538.

Yu, T.-Y., M. B. Orescanin, C. D. Curtis, D. S. Zrnić, and D. E. Forsyth, 2006: Beam multiplexing using the phased-array weather radar. *J. Atmos. Oceanic. Tech.*, **24**, 616–626.

Zhang, G. and R. J. Doviak, 2007: Spaced-antenna interferometry to measure crossbeam wind, shear and turbulence: Theory and formulation. *J. Atmos. Oceanic. Tech.*, **24**, 791–805.

Zhang, G. and R. J. Doviak, 2008: Spaced-antenna interferometry to locate sub-volume inhomogeneties of reflectivity : An anology with monopulse radar. *J. Atmos. Oceanic. Tech.*, **21**, 1921–1938.

Zrnić, D. S., et al., 2007: Agile beam phased array radar for weather observations. *Bull. Amer. Meteor. Soc.*, **88**, 1753–1766.